IPPLM Hall Effect Thruster - design guidelines and preliminary tests

IEPC-2011-221

Presented at the 32nd International Electric Propulsion Conference,
Wiesbaden, Germany
September 11–15, 2011

Jacek Kurzyna* and Dariusz Daniłko†
Institute of Plasma Physics and Laser Microfusion, Hery 23, 01-497 Warsaw, Poland

A small (~ 300 W) Hall effect thruster (HET) was designed and assembled at the Institute of Plasma Physics and Laser Microfusion (IPPLM) in Warsaw, Poland with a view to optimizing its performance for krypton operation. The paper outlines the main objectives and presents the scope of the experiment. The design of the thruster along with the results of numerical modeling and preliminary experimental data are presented. Analytical approximations of magnetization curves of ARMCO iron as well as of radiative heat transfer were incorporated into numerical models in order to obtain more accurate results.

Nomenclature

H	=	magnetizing field [A/m]
B	=	magnetic field [T]
B_{sat}	=	saturation level [T]
r_{L}	=	Larmor radius [mm]
Z_1	=	bottom of the ionization chamber [mm]
Z_2	=	top of the ionization chamber [mm]
R_1	=	inner radius of the ionization chamber [mm]
R_2	=	outer radius of the ionization chamber [mm]
$D = 2R_2$	=	outer diameter of the ionization chamber [mm]
$d = R_2 - R_1$	=	ionization chamber width [mm]
I_{inn}	=	current in the inner coil [A]
I_{out}	=	current in the outer coil [A]
I_{sp}	=	specific impulse [s]

Introduction

XENON is usually regarded as the propellant of choice for ion and Hall effect thrusters (HET). However, the cost of xenon is very high, what is a result of both its low abundance in the Earth's atmosphere (0.087 ppm) and the way it is produced (by fractional distillation of the air). That is why less expensive and more easily ionized elements than xenon are often considered as alternative fuels for electric propulsion devices. In the context of replenishment of the propellant during interplanetary missions, the abundance of appropriate substances in the natural environment of the target planet may also be a significant factor.[1] A critical comparison of several propellants, indicating the most attractive ones in terms of economy, thrust, specific impulse, efficiency, ionization costs, wall erosion, interaction with the spacecraft surface etc., has

*Research Scientist, Division of Magnetised Plasma, jacek.kurzyna@ipplm.pl
†Assistant, Division of Magnetised Plasma, dariusz.danilko@ipplm.pl

been presented e.g. by Kieckhafer.[2] However, technological limitations that usually appear while using solid or chemically active materials may suppress the potential benefits. That is why, the next lighter noble gas - krypton, with its atomic mass of 83.8 u versus 131.3 u of Xe and ionization potential of 14.0 eV instead of 12.1 eV of Xe - is often considered to be a worthy substitute for xenon. The cost of krypton, with its abundance in the air of 1.14 ppm, is about 6 times lower than that of xenon.

The advantages and disadvantages of using krypton as HET propellant have been widely discussed in the literature and are exhaustively summarized by Linnell[3] and Scharfe.[4] Besides economical incentives raised in favor of krypton, there is a number of theoretical advantages related to the lower discharge voltage required for a given specific impulse I_{sp}. That, for instance, might allow a higher I_{sp} to be achieved before wall losses become significant as a result of high electron temperature.[5] The cited papers[2–4] allow us to draw the conclusion that by using krypton one can avoid performing excessive modifications to the HET design (provided that it is already optimized for xenon) as well as facing a number of disadvantages stemming from using substances other than noble gases as a propellant (e.g. deposition of metal vapors at the surface of the spacecraft and/or its solar panels).

After analyzing all the pros and cons with respect to economy, efficiency, and the needs of a potential missions, as well as facing limited funds, the vacuum system of modest efficiency and the need to design the thruster from scratch, the arguments in favor of krypton had prevailed when the decision to develop HET at IPPLM was made. The assumed size and power of the thruster is somehow comparable with the well-known xenon SPT50 model.

I. Design overview

Most analyzes of krypton operation are usually formulated in terms of efficiency, specific impulse, heat loads, magnetic field topology etc., using state-of-the-art xenon HET as a reference for comparisons. It should be noted that scaling laws and numerical modeling results are verified experimentally using thrusters designed and optimized primarily for xenon, whereas the ionization rate of krypton at comparable plasma density and temperature is about 30% lower than that of xenon. (Sometimes, to improve the ionization factor, the increase of discharge channel length is advised. However, it may result in higher particle losses at the channel walls.) In order to reach thruster efficiencies on par with xenon it is usually suggested to maintain the mass flow rate at the same level (thus increasing plasma number density) and to increase the discharge voltage so that to compensate for the lower ionization cross sections. The numerical calculations of Scharfe[4] with the use of 2D hybrid code elaborated for Stanford Hall thruster confirms the validity of such general guidelines. However, keeping the same mass flow rate for krypton (i.e. increasing neutral particle flow rate) and increasing the discharge voltage results in the growth of both, the specific impulse and the discharge current, and therefore, in a drastic increase of heat loads. This imposes strong limitation on the achievable particle flow rate, which may explain the relatively low mass utilization, usually reported for thrusters that use krypton as a propellant.

The reduction of relatively high krypton jet divergence may require further increase of $\mathbf{B}$ as well as optimization of magnetic field topology to make the magnetic mirror effect more prominent.[3,4] Taking the above rationales into consideration and choosing a small ($\sim 0.3 - 0.5$ kW) krypton HET as a baseline, the following design objectives have been specified and accomplished:

- the nominal gas flow rate should be at least 5 times smaller than that of a SPT100 class HET. This way IPPLM vacuum facility with chamber of 3.5 m^3 and system of turbomolecular pumps should ensure the ultimate pressure in the range of about $6 \times 10^{-5} - 1.2 \times 10^{-4}$ Torr for krypton mass flow rate from 1 to 2 mg/s. (However, it is intended to add cryogenic pumps in the future, which should decrease ultimate pressure to $\sim 6 \times 10^{-6}$ Torr for 1 mg/s krypton mass flow rate and make operation with higher flow rates possible).

- A discharge channel outer diameter D of 50 mm and channel width d of 8 mm were assumed (in this way, the channel cross section is scaled down in the same ratio as the gas flow rate). The channel length can be varied in the range of $12 - 35$ mm by adjusting the position of a stainless steel anode inside the insulator with respect to thruster's exit plane. (The anode operates simultaneously as krypton distributor.) For the need of constructing a prototype, alumina insulator was manufactured.

- To supply IPPLM Hall thruster, dedicated power units and gas feeding system were manufactured. As an electron source, commercially available hollow cathode is adopted.

- Following "photographic scaling" and adopting so-called "G criterion,"[6–8] the topology of magnetic field was modeled with the use of Finite Element Method Magnetics (FEMM) freeware package.[9] Several configurations of magnetic circuit were considered. The optimization with respect to "G criterion" was implemented into FEMM calculations using Lua scripting language as described in Sect. III.

- The magnetic circuit design is derived from classic configuration with inner and outer magnetic coils. In the second variant, the inner coil is replaced with permanent magnet (Sm-Co alloy). For further cost reduction, soft iron of ARMCO type was used instead of Fe-Co alloy. Modular design ready to operate with magnetic poles of distinct geometries was manufactured. Using the set of poles prepared in advance, the best topology of magnetic field will be determined in experiments with an operating thruster. The map of magnetic field reproduced in Sect. III was prepared using measurements for the thruster fixed to the laboratory bench.

- It is assumed that the heat excess released in the thruster body can be transferred to the back of the magnetic circuit with the heat guides which are installed inside the thruster body. These heat guides operate simultaneously as thermal shields that prevent most sensitive parts of the magnetic circuit from overheating. Finally, heat energy collected at the back of the thruster is partially radiated but mostly transferred to the dedicated radiator by external heat guides. Figure 1 shows the IPPLM Hall effect thruster attached to the copper radiator and a mounting rack. The effectiveness of the cooling system was modeled with the use of FEMM heat module and confirmed using CRATHER code[10] as described in Sect. II.B.

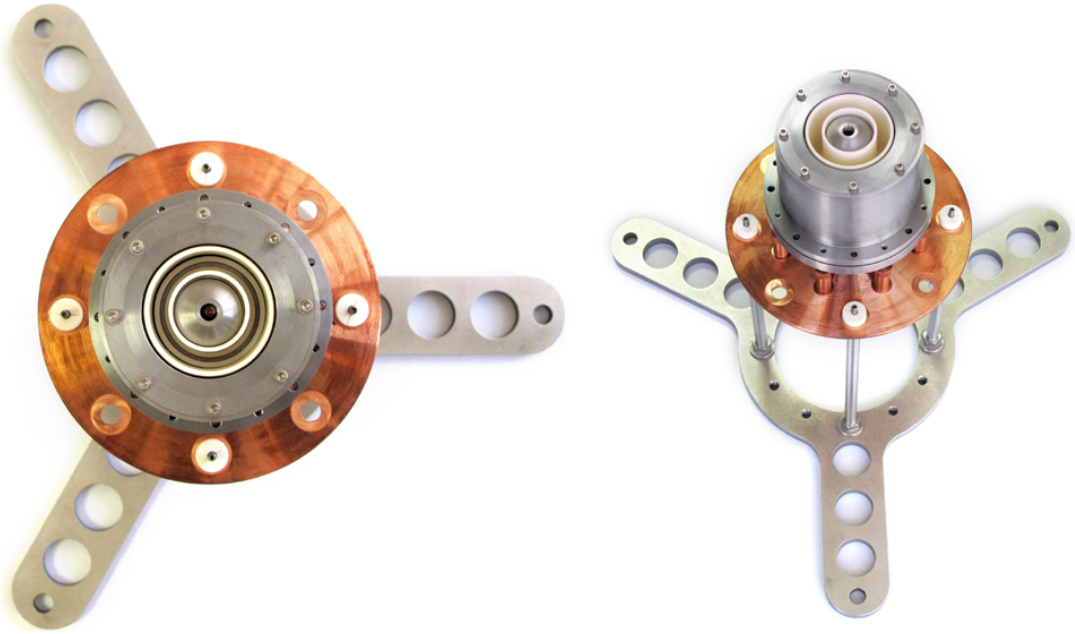

Figure 1. Photos of IPPLM krypton HET - the cathode is disassembled.

II. Numerical modeling

The design described in Sect. I is a result of an extensive research employing thorough numerical investigation. FEMM code was used for modeling both magnetic field topology and temperature distribution. In order to obtain reliable data, material properties had to be chosen accurately. A standard FEMM distribution comes with an extensive library of material properties. However, some of the materials used in the design of the thruster were not rendered in this collection.

A. Magnetic field

Due to the lack of experimental data concerning temperature dependency of the shape of the magnetization curve for iron, we created an empirical model that reproduces such a dependency. Relying upon fragmentary data[9,11] we approximated iron's magnetization curve with a natural logarithm:

$$B(H) = B_{sat} \cdot c_1 \cdot log(c_2 \cdot H) \ , \tag{1}$$

where $c_1 = 0.085$ and $c_2 = 30$.

Such an approximation enables us to modify the shape of the magnetization curve by changing saturation level, B_{sat}, which in this case serves as a free parameter. By doing so, we are able to model magnetic properties of iron at various temperatures while preserving the general character of the curve. The comparison of experimental data with empirical model is presented in Fig. 2. The main advantage of using the empirical model is the fact that it can be fine-tuned to fit reliable experimental data, making numerical simulations even more accurate.

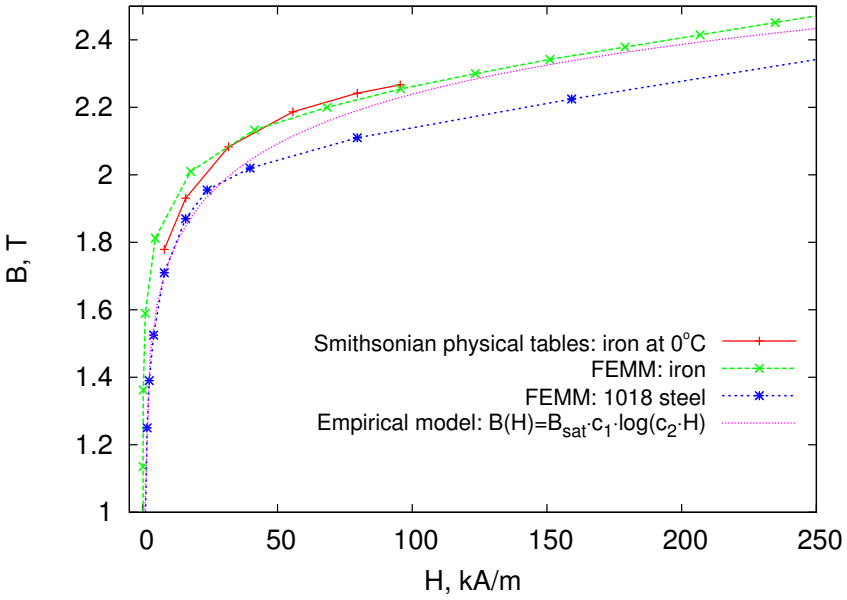

Figure 2. Comparison of magnetization curves based on experimental data[9,11] and on empirical model of Eq. 1 with $B_{sat} = 2.5$ T.

B. Temperature

In order to verify whether the materials selected for manufacturing the thruster would endure severe operational conditions we numerically modeled the temperature distribution in a thruster. Two numerical codes were used for this this purpose: FEMM and CRATHER.

Since FEMM does not include radiative heat transport, which for high vacuum conditions becomes an important way of transferring energy, we had to approximate it using conduction. For this purpose we filled vacuum areas with a virtual material with variant conductivity depending on r. The result of the simulation is presented in Fig. 3 (left).

Due to FEMM's limitations we decided to verify the results with another numerical code capable of solving 2D heat conduction problem, namely: CRATHER. In contrary to FEMM, CRATHER has a well-defined radiative heat transfer, and so, no approximations had to be made in this regard. Figure 3 (right) shows the outcome of the simulation.

As we can see in Fig. 3, the results provided by the two codes are similar, which yields that our original approximation using FEMM code was satisfactory. To maintain low temperature of the insulator and magnetic components, special heat-guiding system was designed, which transfers energy to the copper radiator located at the back of the thruster, thus cooling the entire system. As a result, the temperature is well below the Curie point of the ARMCO iron, which guarantees safe operation.

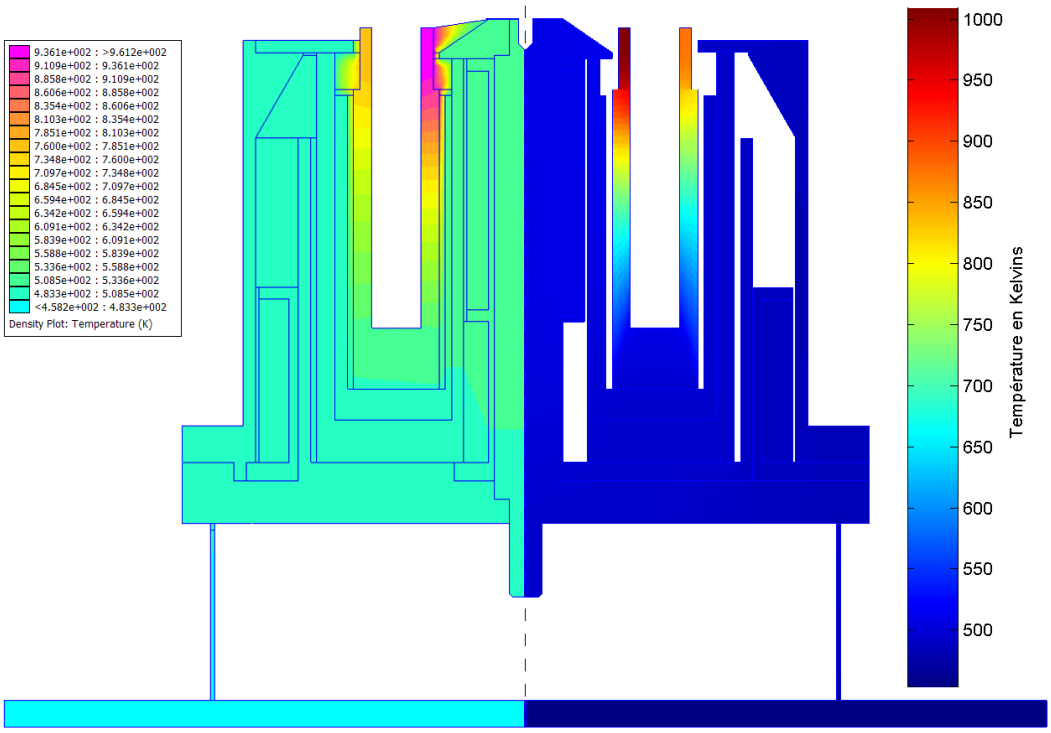

Figure 3. Comparison of numerical modeling of the temperature distribution using FEMM (left) and CRATHER (right) codes.

III. Magnetic field

Magnetic field plays a crucial role in a Hall effect thruster. Not only does it enable Hall current to emerge, but it also traps electrons, thus making effective ionization of the propellant possible. In order to obtain maximal efficiency of the thruster, a proper magnetic field configuration has to be achieved. Its magnitude and topology has to be adjusted so that it efficiently traps electrons ($r_L << d$) and so that it does not affect ions, allowing them to leave the thruster ($r_L >> d$) at the same time. As described in Sect. II.A, FEMM code was used for designing the magnetic circuit of the Hall thruster.

The final version of the thruster enables magnetic field to be modified in two ways: first, by changing currents in coils and second, by using different magnetic circuit setups, as some of its elements were manufactured in different shapes and sizes. What is more, the thruster was built with the possibility to operate it in two different modes: a coil-coil mode and a coil-magnet mode, in which the internal coil is replaced with a permanent magnet. However, from now on we will discuss only the coil-coil mode as no experimental data have been collected for the coil-magnet setup so far.

A. Magnetic field optimization

In order to minimize electron losses to the walls, the magnetic field should form so-called magnetic bottle in order to keep electrons from hitting the walls.

If the pitch angle (θ) of electron's trajectory is too small, it will presumably hit the wall. Therefore, the criterion for confinement is given as:[12]

$$\sin\theta_0 = \sqrt{\frac{B_0}{B_{\text{wall}}}}\ . \tag{2}$$

Here θ_0 is the smallest pitch angle at which an electron is considered confined, B_0 is magnetic field at the location of an electron and B_{wall} is magnetic field at the intersection of corresponding magnetic field line with the wall.

1. *G criterion*

For the purpose of optimizing magnetic field topology in the thruster, we incorporated so-called "G criterion." Blinov et al.[6] suggested to use the following function in order to find the magnetic field topology corresponding to the smallest electron losses at the walls:

$$G = 4\pi \int_{Z_1}^{Z_2} \int_{R_1}^{R_2} \Omega(r,z) dz dr. \tag{3}$$

Here $\Omega(r,z)$ is a cone angle external to the loss cone angle defined in Eq. (2) and equals:

$$\Omega(r,z) = 4\pi \sqrt{1 - \frac{B_0(r,z)}{B_{\text{wall}}(r,z)}}\ . \tag{4}$$

In order to minimize electron losses to the walls, the value of the G function of Eq. (3) should be maximized. Belikov et al.[7] modified Eq. (3) by utilizing the following function F:

$$F = \left| \frac{\mathbf{B} \times \nabla |\mathbf{B}|}{|\mathbf{B}|} \right| \tag{5}$$

as a weight function, obtaining the following criterion for optimal magnetic field:

$$G^* = \frac{\int_{Z_1}^{Z_2} \int_{R_1}^{R_2} F(r,z)\Omega(r,z) dz dr}{4\pi \int_{Z_1}^{Z_2} \int_{R_1}^{R_2} F(r,z) dz dr}. \tag{6}$$

With the use of FEMM code and self-developed Lua scripts, we performed a series of numerical experiments in order to find optimal values of thruster's parameters. Calculations performed with the use of "G* criterion" of Eq. 6 enabled us to identify which of the magnetic circuit designs and what currents in thruster's coils provide the most effective trapping of electrons. The distribution of magnetic field lines corresponding to the minimal electron losses is presented in Fig. 4.

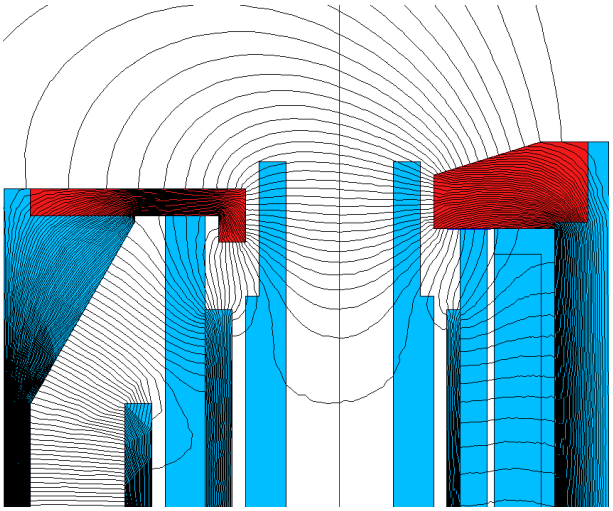

Figure 4. Optimal topology of the magnetic field obtained numerically with the use of the "G* criterion." Numerical results enabled choice of some of the magnetic elements (red) and currents in coils to be: $I_{inn} = 1$ A, $I_{out} = 0.5$ A.

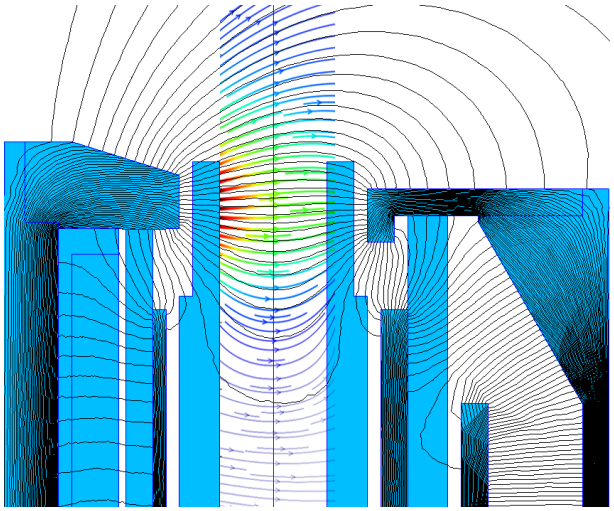

Figure 5. Comparison of magnetic field topology obtained experimentally (colorful lines) and numerically (black lines) for currents: $I_{inn} = 1$ A, $I_{out} = 0.5$ A.

2. *Measurements of the magnetic field*

In order to verify numerical results we measured magnetic field distribution of the thruster with the use of the RX25 Resonance Technology teslameter equipped with a 3D probe, designed especially for this purpose.

The thruster was mounted on a laboratory bench and the measurements were taken with a not-in-operation thruster under atmospheric pressure.

Measured data served firstly to fine-tune the profile of iron's magnetization curve used in FEMM simulations by setting $B_{\mathrm{sat}} = 2.3\,\mathrm{T}$ in Eq. (1). Experimental data were then compared with the updated numerical results as presented in Fig. 5. We can see that the agreement is very good, what implies that we have two independent and very reliable sources of information on magnetic field topology. Empirical verification of the applicability of the G criterion to the newly developed Hall thruster is one of the objectives of the experiment and will be studied further. Figure 6 represents experimental profile of B_{r} along the channel.

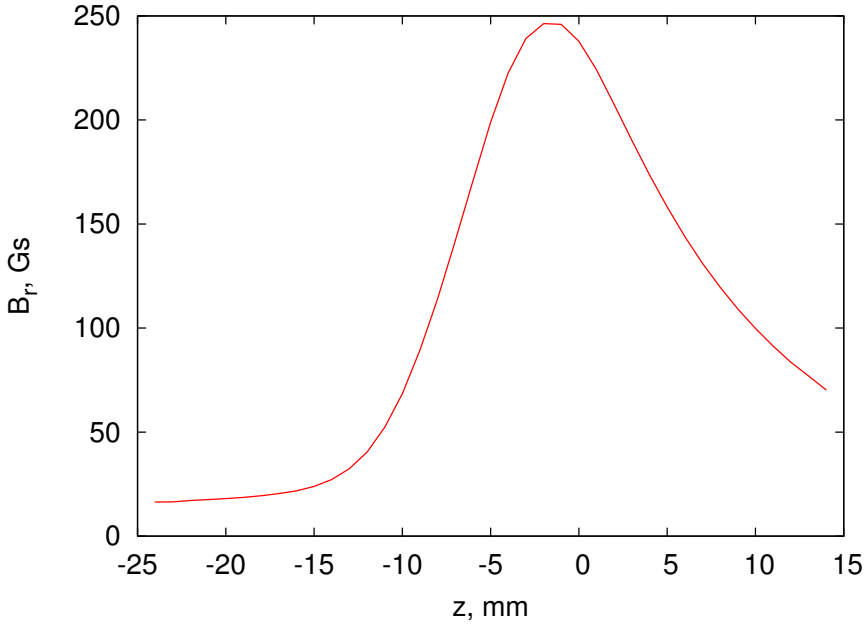

Figure 6. Profile of B_r along the ionization channel (based on experimental data).

IV. Summary

The main objective of the experiment is to develop a 0.3kW Hall thruster and optimize its performance for krypton operation. The thruster has been designed following "photographic scaling" laws and in accordance with various numerical results. It has been manufactured as a modular construction, enabling various modifications to be performed during testing, including:

- changing the length of the ionization chamber by altering the position of the anode,
- testing various magnetic circuit setups (several configurations with different magnetic poles and a mode with permanent magnet).

The aim of incorporating these modifications is to maximize thruster's efficiency.

The preparation stage of the experiment is finalized and the thruster is designated for testing in a vacuum chamber. Operational characteristics will be completed and analyzed in the near future. This should provide an $I-V$ map for different krypton flow rates. Additionally, the "G criterion" will be verified experimentally by estimating the influence of various magnetic setups on thruster's efficiency.

The studies on Hall plasma accelerators at IPPLM aim not only at space propulsion applications but also at searching new technologies which could be useful for material processing in high power plasma facilities (e.g. release of material deposited in discharge chamber walls). From this point of view, feeding Hall thrusters with krypton and finally with lighter and possibly reactive gases seems to be a promising research area.

Acknowledgments

The authors are indebted to Serge Barral for a number of profitable discussions and support with numerical codes CRATHER and HETMAN, as well as to Marek Scholz for his permanent assistance and favor. The project is supported within the frame of IPPLM statutory activity.

References

[1]Hopkins, M. A., Makela, J. M., Washeleski, R. L., and King, L. B., "Mass Flow Control in a Magnesium Hall-effect Thruster," *Proc. 46th AIAA Joint Propulsion Conference*, No. 10-6861, American Institute of Aeronautics and Astronautics, Washington, D.C., 2010.

[2]Kieckhafer, A. and King, L. B., "Energetics of Propellant Options for High-Power Hall Thrusters," *Proc. of the Space Nuclear Conference*, No. 1025, 2005.

[3]Linnell, J. A., *An Evaluation of Krypton Propellant in Hall Thrusters*, Ph.D. thesis, Aerospace Engineering, The University of Michigan, 2007.

[4]Scharfe, D. B., *Alternative Hall Thruster Propellants Krypton and Bismuth: Simulated Performance and Characterization*, Ph.D. thesis, Mechanical Engineering, Stanford University, 2009.

[5]Gascon, N., Dudeck, M., and Barral, S., "Wall Material Effects in Stationary Plasma Thrusters. I. Parametric studies of an SPT-100," *Phys. Plasmas*, Vol. 10, 2003, pp. 4123.

[6]Blinov, N. V., Gorshkov, O. A., and Shagayda, A. A., "Experimental Investigation of Magnetic Field Topology Influence on Structure of Accelerating Layer and Performance of Hall Thruster," *Proc. 29th International Electric Propulsion Conference*, No. 05-033, The Electric Rocket Propulsion Society, Worthington, OH, 2005.

[7]Belikov, M. B., Gorshkov, O. A., Dyshlyuk, E. N., Lovtzov, A. S., and Shagayda, A. A., "Development of Low-Power Hall Thruster with Lifetime up to 3000 Hours," *Proc. 30th International Electric Propulsion Conference*, No. 07-129, The Electric Rocket Propulsion Society, Worthington, OH, 2007.

[8]Gorshkov, O. A. and Shagaida, A. A., "The Criterion of Optimal Configuration of Magnetic Field in a Thruster with Closed Electron Drift," *High Temp.*, Vol. 46, 2008, pp. 529.

[9]Meeker, D. C., "Finite Element Method Magnetics," http://www.femm.info, Version 4.2 (09Nov2010 Build).

[10]Barral, S. and Brayer, C., "CRATHER: un Code de Conduction-RAdiation THERmique," Tech. rep., CNRS, 1997.

[11]Smithsonian Institution and Fowle, F., *Smithsonian physical tables*, Smithson. Inst., 1916.

[12]Chen, F. F., *Introduction to Plasma Physics and Controlled Fusion*, Vol. 1, Plenum Publishing Corporation, 1984.